SAKARYA ÜNİVERSİTESİ
FEN BİLİMLERİ ENSTİTÜSÜ DERGİSİ

Sakarya University Journal of Science
SAUJS

ISSN 1301-4048 e-ISSN 2147-835X Period Bimonthly Founded 1997 Publisher Sakarya University
http://www.saujs.sakarya.edu.tr/

Title: Estimating the Strength and Deformation Properties of the End Milling Process Using Numerical Analysis Methods

Authors: Yasin Furkan GÖRGÜLÜ, Murat AYDIN

Recieved: 2023-02-01 00:00:00

Accepted: 2023-03-06 00:00:00

Article Type: Research Article

Volume: 27
Issue: 3
Month: June
Year: 2023
Pages: 580-589

How to cite
Yasin Furkan GÖRGÜLÜ, Murat AYDIN; (2023), Estimating the Strength and Deformation Properties of the End Milling Process Using Numerical Analysis Methods. Sakarya University Journal of Science, 27(3), 580-589, DOI: 10.16984/saufenbilder.1245764
Access link
https://dergipark.org.tr/en/pub/saufenbilder/issue/78131/1245764

Sakarya University Journal of Science 27(3), 580-589, 2023

Estimating the Strength and Deformation Properties of the End Milling Process Using Numerical Analysis Methods

Yasin Furkan GÖRGÜLÜ *[1], Murat AYDIN[1]

Abstract

In the study, the end mill made of titanium material and having a unique design with a 4-flute was simulated during the milling of the workpiece with a geometry of a rectangular prism made of aluminum material. Ansys Explicit Dynamics was used in the study. Modeling and simulation of the milling process were made with finite element analysis for the estimation of the strength properties. The end mill is chosen as a titanium alloy, while the milled workpiece is aluminum. All parameters were kept constant and only the depth of cut was examined in three scenarios 3, 6, and 9 mm. The simulations were carried out by taking the spindle speed of 4000 RPM and the feeding rate of 3350 mm/s. One of the conveniences provided by Explicit Dynamics is that it can be solved in very small time intervals, and for this reason, the time step in the analysis is solved by taking 0.001 seconds. While hexahedral mesh is applied to the tool, a tetrahedral mesh is applied to the workpiece. The generated mesh has 8,012 nodes and 17,052 mesh elements. Average deformations for both tool and workpiece are 36.92, 38.10, and 38.29 mm, respectively. Strain also shows a similar trend to the total deformation and the average values for all three scenarios were found to be 2.84 x 10^{-3}, 4.43 x 10^{-3} and 3.99 x 10^{-3} mm/mm. Also, the stress values were obtained as 78.23, 76.83, and 77.99 MPa.

Keywords: Ansys, deformation, end mill, explicit dynamics, stress and strain.

1. INTRODUCTION

In industrial applications, machining can be done in several ways such as turning, drilling, grinding, milling and so on. But, there are some challenges such as stress formation that milling (a trustable way of production of structures or parts) has to defy [1]. In milling operation, cutters are the essential elements of material processing and have different geometries or profiles. There are plenty of studies that evaluated milling experimentally and/or numerically. The following studies are focused on the finite element modeling and analysis of the end milling applications using different tools and materials.

It was verified the cutting tool forces and stresses for milling Titanium alloy Ti-6Al-4V cut by a tungsten carbide end mill [2]. It was calculated the temperature fields in the tool and workpiece [3]. It was predicted the milling forces on the processing of aluminum alloy 7050 [4]. There are studies that evaluate the influence of cryogenic cooling on the

* Corresponding author: yasingorgulu@isparta.edu.tr (Y. F. GORGULU)
[1] Isparta University of Applied Sciences, Keciborlu Vocational School, Isparta University of Applied Sciences, Isparta, Turkey.
E-mail: murataydin@isparta.edu.tr
ORCID: https://orcid.org/0000-0002-1828-2849, https://orcid.org/ 0000-0002-3015-1868

cutting temperature, forces, and chip formation on the micro-milling of Ti6Al4V [5]. Kumar and Srinivas evaluated the burr formation while small-milling of an Al6061-T6 by flat end mill with small cutters and varying geometry of the tools [6].

Praven and Elaya predicted the delamination behavior of Glass Fiber Reinforced Plastics (GFRP) while milling using a K10 end mill (carbide tool coated with Titanium nitride having four flutes each with square ends) and stated that the finite element analysis (FEA) provided close results to the experimental ones [7]. It was evaluated the cutting forces and tool tip displacement for end milling processes [8]. Prasad and Sreedhar predicted deformation and stress properties of the Tungsten Carbide tool while slow, medium, and high-speed cutting of aluminum alloy Al6061-T6 [9].

There are also studies evaluate the stress value and tool displacement in the cutting tool (TiAlN) during hard end milling of heat-treated low alloy steel (42CrMo4) [10]. It was evaluated the surface properties of thin-wall workpieces due to thermo-mechanical deflection while machining. Karidkar and Patankar [11] evaluated the machining of thin wall machining of Al8011 and stated that experimental deformation values can be well predicted (from 1.8 to 12.8% diffractions, 6.2% avg.) by FEM&A. Işık and Öztürk [12] predicted the influences of cutting speed and feed rate on the cutting forces (total deformation and von Mises stresses) while drilling holes on AISI 140 using TiAIN-coated hard carbide cutting tool. Kumar and Mall [13] evaluated the vibration behavior of high speed steel (UNST11302) single point cutting tool in turning operation. Rajpoot and Siddique [1] predicted the stress formation on the end mill cutters with varying geometry during the milling operation of AlSi 1045. It was studied the tool particle interaction and stress distribution in particles along, above, and below the cutting path under different cutting speeds and constant depth of cut while machining discontinuously reinforced aluminum composites made of 6061 aluminum alloy and 25 micron silicon carbide particles [14]. It was modeled an end mill with a damper for reducing the vibration while high-speed milling application [15].

Mustapha and Zhong analyzed the transverse vibration behavior of a micro end mill [16]. It was evaluated the depth of feed on the stress of the end mill [17]. It was evaluated the deformation of a four-flute mill [18]. Tandon and Khan [19] modeled a flat end mill (A four-fluted M42 high-speed steel with a 30° helix angle) and predicted stress distribution (von Mises stress), translational displacement, and deformation values. Yang and Zheng [20] used deform three-dimensional FEA for simulation of ball-end milling of hardened (42HRC, 52HRC, and 62HRC) workpieces (Cr12MoV) and evaluated the milling forces and stress and temperature distributions.

It was designed an end mill to optimize the structure of a variable pitch end mill for achieving better vibration and stability performances [21]. It was evaluated the influence of spindle speed and cutter length on the stress and strain values of the micro-milling cutter (2 flutes) [22]. It was predicted the cutting force while end milling of 42CrMo4 steel (40HM) [23]. When the literature was reviewed, it was seen that influence of cutting depth on the total deformation, strain, and stress of the cutter is not dynamically evaluated by explicit dynamics. Indeed, the most essential parameters that influence the stress value and tool displacement during the machining in entire machining conditions are cutting speed and depth, and machining time [10]. Therefore, this study tried to figure out this issue by numerical analysis using a unique design cutter with four-helix flutes.

2. MATERIALS AND METHODS

2.1. Tool-workpiece Design

In the study, an end mill made of titanium material [24] with 4 helical flutes was selected and designed. The total length of the end mill is 92 mm, and the diameter of the cutting edge, and the shank are 16 mm. The usable cutting length with a specified number of teeth is designed as 38 mm. It also has a helix angle of 25° for general machining purposes [25]. Tool material has a density of 4510 kg/m^3 and a specific heat value of 500 J/kg.°C. It starts the cutting process by face milling and outside the workpiece as shown in figure 1. The workpiece is Al 1100-O material with a density of 2707 kg/m^3 and a specific heat of 884 j/kg.°C [24]. The end mill was chosen as a brittle material, while the workpiece was chosen as a ductile material. The dimensions of the workpiece are designed as 28, 50, and 20 mm in width, length, and height, respectively.

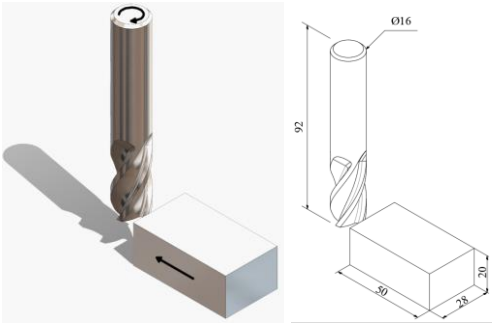

Figure 1 The three-dimensional end mill and workpiece models with dimensions.

2.2. Finite Element Analysis Using Explicit Dynamics

The mathematical description of a physical system that includes a part or assembly, material characteristics, and boundary conditions are called FEA. It is not always possible to estimate product behavior in the actual world using straightforward calculations. By precisely describing physical processes using partial differential equations, a generic methodology like FEA offers an easy way to express complex behaviors. Design engineers and professionals can utilize FEA now that it has developed and become more accessible [26]. FEA was carried out using the Explicit Dynamics tool of the Ansys software. Explicit dynamics, which is a branch of the finite element method, was used in the study. Here, the chip removal process of the end mill cutter from the workpiece was simulated.

The end mill cutter and workpiece modeling were made using a commercial computer-aided design (CAD) program called SolidWorks. Afterward, CAD designs were transferred to the Explicit Dynamics section under Ansys Workbench. One of the distinguishing differences between Explicit Dynamics and Implicit Dynamics is that they can analyze very small time intervals [27]. The time interval of the analysis made in the study was resolved as 0.001 seconds. A hexahedral mesh structure was created on the end mill and a tetrahedral mesh structure on the workpiece. The mesh has a total of 17052 mesh elements, 8012 nodes and it is demonstrated in Figure 2. Mesh quality is an important factor in terms of the accuracy of results in FEA studies. For this reason, skewness, orthogonal quality, and aspect ratio, which are 3 parameters that are important in mesh quality, were checked.

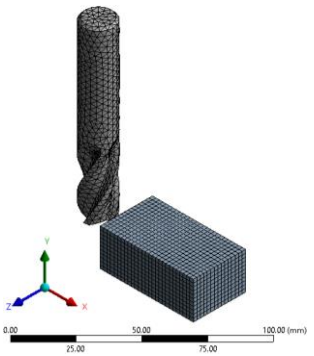

Figure 2 The mesh structure of the end mill and workpiece.

The average skewness of the generated mesh is 0.2014. Mesh quality in the range of 0 to 0.25 on the scale shared by Ansys is defined as “Excellent” [28–32]. The average orthogonal quality, which is the second quality indicator, is 0.79728. This ratio between 0.70 and 0.95 is defined as “Very

Good". The third parameter, aspect ratio, is recommended to be less than 20 and it is 1.6918 in the analysis. The aforementioned skewness and orthogonal quality ratios are given in tables 1 and 2.

Separate displacements have been defined for the tool and the workpiece. While the end mill rotates clockwise with 4000 RPM, the workpiece advances towards the end mill at 3350 mm/s (see figure 1.). After the start of the cutting process, the end mill cutter rotates to cut the workpiece along its length. The quality scale of these two parameters is given in Tables 1 and 2 [28–32].

Table 1 The skewness mesh quality metrics spectrum.

Excellent	Very good	Good	Acceptable	Bad	Inacceptable
0.00-0.25	0.25-0.50	0.50-0.80	0.80-0.94	0.95-0.97	0.98-1.00

Table 2 The orthogonal quality mesh metrics spectrum.

Inacceptable	Bad	Acceptable	Good	Very good	Excellent
0.000-0.001	0.001-0.100	0.100-0.200	0.200-0.690	0.700-0.950	0.950-1.000

The study done can be categorized as groove cutting and side cutting. Formulas used in end milling calculations are as follows [33–36]:

$$v_C = \frac{\pi \times D_C \times n}{1000}$$

Where:
v_C: cutting speed
D_C: end mill diameter
n: spindle speed

$$v_f = n \times f \quad (2)$$

Where:
v_f: feed rate
f: feed rate per tooth

3. RESULTS AND DISCUSSION

In the study, it was simulated that a 4-flute end mill cuts the workpiece from one end to another at different depths of cut. As a result of the simulation, the total deformation, strain, and stress ratios were examined and these were graphed comparatively. Graphs of these parameters are shown for end mill and workpiece (figures 3.-5.), end mill only (figures 6.-8.), and workpiece only. In figures 3.-5., the visuals have been strengthened with the simulation images of the tool and the workpiece. The 0.001-second simulation was divided into 20 equal time steps and the time steps after the end mill has completely cut the workpiece are excluded from the charts. Thus, after the 0.00055th second, it is not shown in the graphics.

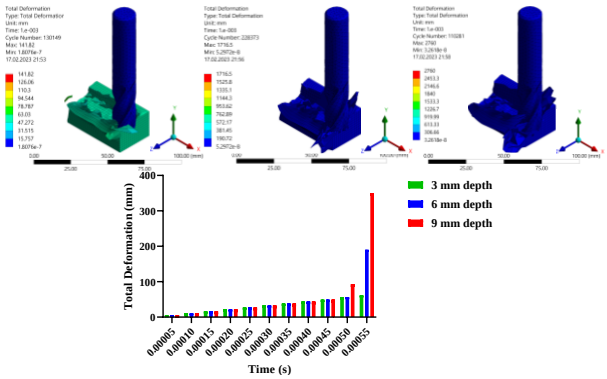

Figure 3 Total deformation amounts and scene images according to 3, 6, and 9 mm cutting depths, respectively.

A gradual increase in total deformation is observed for every 3 depths of cut up to the 0.00050th second (figure 3). In this and the next time step, there is an increase in depths of cut of 6 mm and 9 mm. As a result, it is seen that the average total deformation amount reaches 36.92 mm for 3 mm depth of cut, 38.10 mm for 6 mm depth of cut, and 38.29 mm for 9 mm depth of cut. The maximum deformation data appears to be very high and this is because some of the removed chips splash around and reach far.

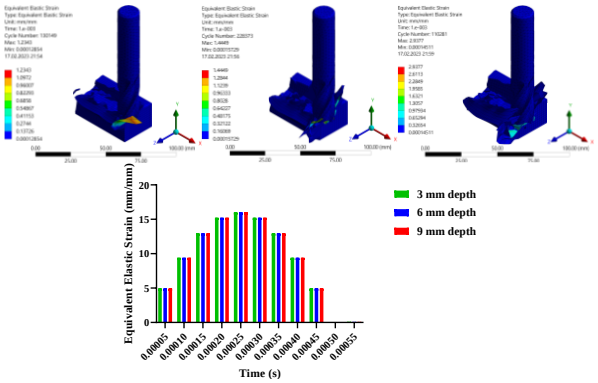

Figure 4 Strain amounts and scene images according to 3, 6, and 9 mm cutting depths, respectively.

The equivalent elastic strain graph for the tool and workpiece is illustrated in figure 4. Elastic strain rates appear relatively low but are normal since the process is geared towards plastic strain. Elastic deformation peaks in the middle of the cutting process and approaches approximately 15 mm/mm. After the peak, a regular decrease is observed. Very small strains occur in the 0.00050th and 0.00055th seconds. It is observed that all strains are very close to each other regardless of the depths of cut.

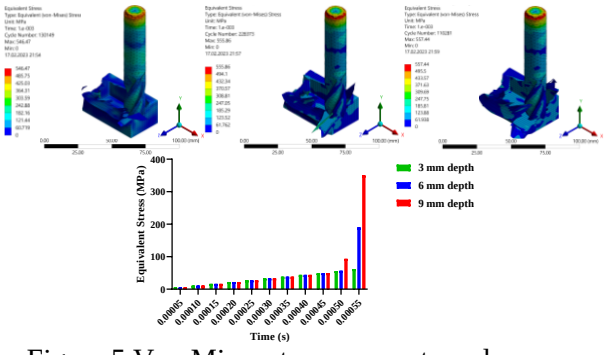

Figure 5 Von Mises stress amounts and scene images according to 3, 6, and 9 mm cutting depths, respectively.

Von Mises stresses in the tool and workpiece are depicted in figure 5 in the MPa unit. Equivalent stress follows the same trend as the graph showing the total amount of deformation for the tool and the workpiece. It shows an increase at the end of the cutting process and the amount of stress increases considerably, especially in the simulation with a cutting depth of 9 mm.

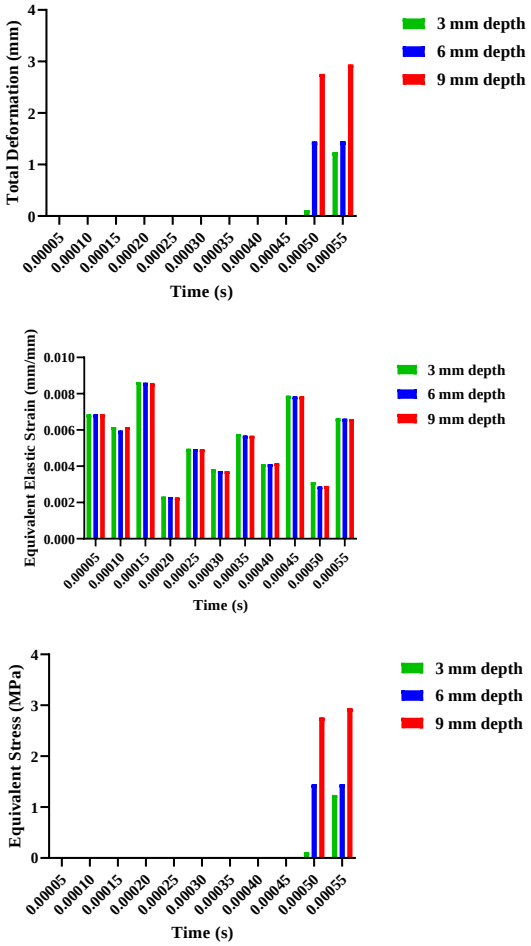

Figure 6 The total amount of deformation, strain and stress occur only in the milling cutter according to the depths of cut of 3, 6, and 9 mm.

Especially the superiority of titanium material over aluminum in the cutting process is seen in figure 6. The 4-flute end mill used in the simulation is not defined as rigid, but is defined as flexible to approach real-life applications. Even if it is small, total deformations in the cutting edge occur especially towards the end of the cutting process.

The strains that occur in the end mill according to different depths of cut are demonstrated in figure 6. Although the strain occurs at very low rates, it follows a fluctuating trend. It is noteworthy that the strain rates of all three scenarios are very close to each other. The reason for the fluctuation is thought to be related to heterogeneous cutting and serrated chip formation.

In the titanium end mill, the greatest stresses occur towards the end of the cut. In the previous time steps, the stress ratios are not visible on the chart because they are much smaller than 1. The greatest stresses occur at the end mill with a depth of cut of 9 mm (see figure 6).

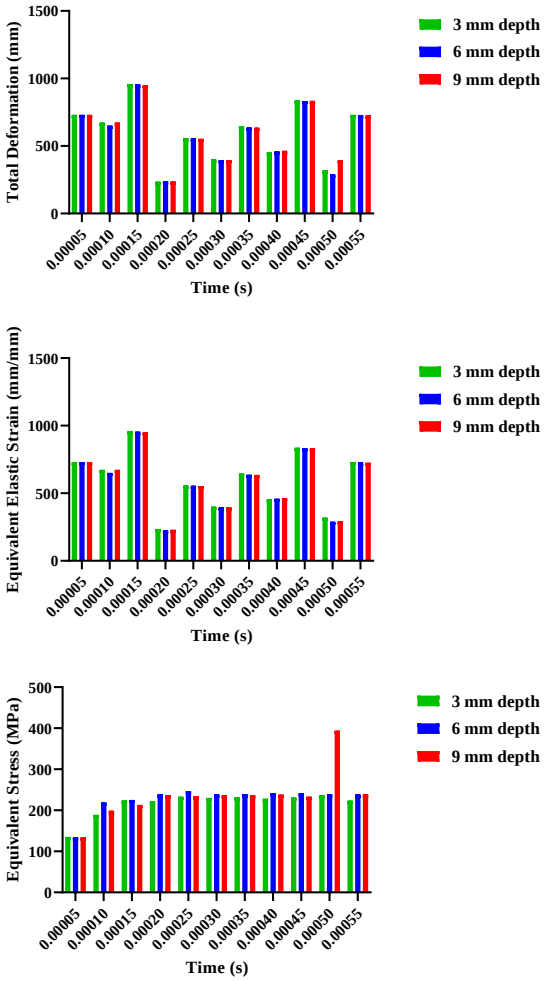

Figure 7 The total amount of deformation, strain and stress occurs only in the workpiece according to the depths of the cut of 3, 6, and 9 mm.

The total deformation of the workpiece is given in figure 7. When the total deformation rates of the workpiece are examined, fluctuating and close to each other rates are observed. Except for the 0.00010^{th} and 0.00050^{th} seconds, the deformation data appear to be almost very close according to the cutting depths.

Figure 7 also shows the strain of the workpiece, but is similar to the general image of figure 6. Minor changes are observed at the 0.00010^{th}, $0.00020^{th,}$ and 0.00050^{th}-time steps compared to the other time steps.

A constant transition is observed in the von Mises stresses of the workpiece, except for two time steps. While the stresses are around 100 MPa in the 0.00005^{th} second, the stress levels approximately double after the end mill is fully inserted into the part and continue to be constant. In the scenario with a depth of cut of 9 mm at 0.00050 seconds, an extreme increase appears. The reason for this is thought to be due to the formation of serrated chips and the inability of the end mill to cut the workpiece properly.

It should be taken into consideration that almost all performed milling trials will adopt dry cutting to prevent the effects of cutting fluid or coolant, which are hard to bear in mind while simulating by FEA [4]. In this study, neither fluid nor a coolant was applied but contrary to this expression, they performed FEA using cryogenic cooling and stated that tool life, dimensional accuracy, and roughness values can be advanced by cryogenic utilization [5].

Cutting depth is one of the most influencing parameters in milling applications. According to FEA results, it was reported that a decrease in cutting depth causes an increase in stress value due to a decrease in the contact zone between the tool and chip [10]. The authors also approved that FEA can be well enough to forecast the stress value and displacement of the cutting tool. As can be seen in the figures 5, 6, and 7, the total amount of deformation and von Mises Stress values were increased with the increase in cutting depth which is opposed to the conclusion of a study [10].

Işık and Öztürk [12] stated that cutting forces increase with the increase in cutting speed and feed rate while removing chips. According to the authors, not only there is a direct interaction between the cutting forces and

total deformation of the tool, but also the von Mises stresses. In this study, speed and feed rate were constant, but should be considered by a future study for comparison.

4. CONCLUSIONS

The simulation of a 16 mm diameter end mill made of titanium material with 4 flutes, which is the cutting tool, cutting the workpiece made of aluminum material was performed using Ansys Explicit Dynamics. As a result of the simulation, the total deformation, strain, and stress values were created according to different depths of cut for all three scenarios. In all three scenarios:

- Serrated chips on the workpiece are noticeable after the milling process. Even if the type and size of the end mill, material kind, and processing parameters such as feed rate and spindle speed were not the evaluated factors, it is thought that these variables have to be optimized for proper milling.
- The average deformations occurring in both the tool and the workpiece were found to be 36.92 mm for 3 mm cutting depth, 38.10 mm for 6 mm, and 38.29 mm for 9 mm.
- Considering the average total elastic strains, values are 2.84 x 10^{-3} mm/mm, 4.43 x 10^{-3} mm/mm, and 3.99 x 10^{-3} mm/mm respectively.
- When the average von Mises stresses are evaluated, it reaches 78.23 MPa for the 3 mm depth of cut scenario, 76.83 for 6 mm, and 77.99 MPa for 9 mm.
- Considering the resulting stresses, the cutting depth of 6 mm, which is the second of the three scenarios, can be stated as the most successful scenario since it has the lowest stress values.

Funding
The authors have not received any financial support for the research, authorship or publication of this study.

Authors' Contribution
The authors contributed equally to the study.

The Declaration of Conflict of Interest/ Common Interest
No conflict of interest or common interest has been declared by the authors.

The Declaration of Ethics Committee Approval
This study does not require ethics committee permission or any special permission.

The Declaration of Research and Publication Ethics
The authors of the paper declare that they comply with the scientific, ethical and quotation rules of SAUJS in all processes of the paper and that they do not make any falsification on the data collected. In addition, they declare that Sakarya University Journal of Science and its editorial board have no responsibility for any ethical violations that may be encountered, and that this study has not been evaluated in any academic publication environment other than Sakarya University Journal of Science.

REFERENCES

[1] I. Rajpoot, S. N. Siddique, "Investigation and numerical analysis of milling cutter," International Research Journal of Engineering and Technology (IRJET), vol. 05, no. 06, pp. 1508–1513, 2018.

[2] V. Kumar, A. Eakambaram, A. Arivazhagan, "FEM analysis to optimally design end mill cutters for milling of Ti-6Al-4V," Procedia Engineering, vol. 97, pp. 1237–1246, 2014.

[3] D. V. Evdokimov, D. G. Fedorov, D. L. Skuratov, "Thermal stress resarch of processing and formation of residual stress when end milling of a workpiece," World Applied Sciences Journal, vol. 31, no. 1, pp. 51–55, 2014.

[4] W. Ma, R. Wang, X. Zhou, X. Xie, "The finite element analysis–based

simulation and artificial neural network–based prediction for milling processes of aluminum alloy 7050," Proceedings of the Institution of Mechanical Engineers, Part B: Journal of Engineering Manufacture, vol. 235, no. 1–2, pp. 265–277, 2021.

[5] M. A. Oymak, E. Bahçe, İ. Gezer, "Investigation Of Cryogenic Cooling Effect With Finite Element Method In Micro Milling Of Ti6al4v Material," International Journal of Innovative Engineering Applications, 2021.

[6] K. K. Kumar, N. Srinivas, "Optimization and Process Control in Small Diameter End Mill," International Journal of Engineering Science and Computing, vol. 6, no. 8, pp. 2581–2585, 2016.

[7] P. Praveen Raj, A. Elaya Perumal, "Prediction of Delamination in End Milling of GFRP Using ANSYS," Asian International Journal of Science and Technology in Production and Manufacturing Engineering, vol. 6, no. 2, pp. 39–46, 2013.

[8] A. C. Araujo, A. M. Savi, P. M. L. C. Pacheco, "Experimental and Numerical Analysis of End Milling," in VI National Congress of Mechanical Engineering, 2010.

[9] S. S. Prassad, C. Sreedhar, "Finate Element Analysis of Multi Point Cutting Tool," ANVESHANA's International Journal of Research in Engineering and Applied Sciences, vol. 1, no. 11, pp. 123–135, 2016.

[10] M. Dragicevic, S. Jozic, D. Bajic, "Finite element simulation of stresses distribution and tool displacement in the cutting tool during hard nd-milling in different machining conditions," in Mechanical Technology and Structural Materials, 2017, vol. 2017, no. 55, pp. 29–36.

[11] S. S. Karidkar, V. A. Patankar, "Finite Element Modeling and Simulation of Thin Wall Machining of Al 8011," International Journal of Engineering Research and Technology, vol. 10, no. 1, pp. 654–658, 2017.

[12] Y. Işık, E. Öztürk, "Experimental Analysis of Cutting Forces and Finite Element Simulation in Milling Operations," International Journal of Mechanical Engineering, vol. 8, no. 11, pp. 1–7, 2021.

[13] V. Kumar, R. N. Mall, "Analysis and Modelling of Single Point Cutting Tool with help of ANSYS for Optimization of Vibration Parameter," International Journal for Scientific Research & Development, vol. 3, no. 9, pp. 175–177, 2015.

[14] R. Shetty, K. Laxmikant, R. Pai, S. S. Rao, "Finite element modeling of stress distribution in the cutting path in machining of discontinuously reinforced aluminium composites," ARPN Journal of Engineering and Applied Sciences, vol. 3, no. 4, pp. 25–31, 2008.

[15] N. H. Kim, D. Won, J. C. Ziegert, "Numerical analysis and parameter study of a mechanical damper for use in long slender endmills," International Journal of Machine Tools and Manufacture, vol. 46, no. 5, pp. 500–507, 2006.

[16] K. B. Mustapha, Z. W. Zhong, "A new modeling approach for the dynamics of a micro end mill in high-speed micro-cutting," JVC/Journal of Vibration and Control, vol. 19, no. 6, pp. 901–923, 2013.

[17] D. R. Pradica, Andoko, D. Z. Lubis, "Simulation on the spindle of a five-

axis multifunctional CNC machine using finite element method," IOP Conference Series: Materials Science and Engineering, vol. 1034, no. 1, p. 012017, 2021.

[18] Q. Liu, H. Xu, J. Wang, "Analysis of four-edge mill modality and stress deformation based on ANSYS," Journal of Physics: Conference Series, vol. 1939, no. 1, 2021.

[19] P. Tandon, M. Rajik Khan, "Three dimensional modeling and finite element simulation of a generic end mill," CAD Computer Aided Design, vol. 41, no. 2, pp. 106–114, 2009.

[20] L. Yang, M. L. Zheng, "Simulation and analysis of ball-end milling of panel moulds based on deform 3D," International Journal of Simulation Modelling, vol. 16, no. 2, pp. 343–356, 2017.

[21] W. Nie, M. Zheng, S. Xu, Y. Liu, H. Yu, "Design and Optimization of Variable Pitch End Mills Based on Dynamic Balance Accuracy," 2021.

[22] X. X. Wang, X. H. Lu, G. H. Xu, F. C. Wang, "The finite element analysis of the stress and deformation of the micro-milling cutter based on ANSYS," Applied Mechanics and Materials, vol. 494–495, pp. 345–348, 2014.

[23] M. Madajewski, S. Wojciechowski, N. Znojkiewicz, P. Twardowski, "Hybrid numerical-analytical model for force prediction in end milling," Mechanik, vol. 91, no. 8–9, pp. 757–759, 2018.

[24] D. Steinberg, Equation of state and strength properties of selected materials. Lawrence Livermore National Laboratory, 1996.

[25] Conical Cutting Tools, "Choosing the Correct Angle End Mill For Your Job," 2023. https://conicalendmills.com/ordering/selection-guide/helical-angle-selection/ (accessed Feb. 16, 2023).

[26] M. Melchiorre, T. Duncan, "The Fundamentals of FEA Meshing for Structural Analysis," 2021. https://www.ansys.com/blog/fundamentals-of-fea-meshing-for-structural-analysis (accessed Jul. 04, 2022).

[27] A. A. Carvalho, "Tips and Tricks for Explicit Simulations," 2019.

[28] Ansys Inc., "Introduction to Ansys Meshing." Ansys Inc., pp. L5-16, 2011.

[29] Ansys Inc., "Mesh Quality And Advanced Topics Ansys Workbench 16.0," 2015.

[30] A. Cambaz, Y. F. Gorgulu, H. Arat, "Analysing fluid-structure interaction with CFD and FEA on a marine double-wall LNG piping system," Multidisciplinary Scientific Journal of Maritime Research, vol. 36, no. 1, pp. 51–60, 2022.

[31] A. Cambaz, Y. F. Görgülü, H. Arat, "Two-Phase Numerical Modelling of a Wet Exhaust System in a Catamaran Motor Yacht Diesel Engine," European Journal of Science and Technology, vol. 31, no. Supp. 1, pp. 165–170, 2021.

[32] Y. F. Görgülü, M. A. Özgür, R. Köse, "NACA 0009 Profilli Bir Kanadin Düşük Bir Reynolds Sayisinda Had Analizi," Journal of Polytechnic, vol. 0900, no. 3, pp. 1237–1242, 2021.

[33] A.L.M.T Corp., "Formula to calculate cutting process," 2022. https://www.allied-material.co.jp/en/products/diamond/knowledge/cutting_formula.html (accessed Jul. 04, 2022).

[34] Helical Solutions, Machining Guidebook. 2016.

[35] J. R. Walker, B. Dixon, Machining Fundamentals, 10th ed. The Goodheart-Willcox Company, Inc., 2019.

[36] E. Oberg, F. D. Jones, H. L. Horton, H. H. Ryffel, C. J. McCauley, Machinery's Handbook, 31st ed. Industrial Press, Inc., 2020.